

Original research article

Role of a-Si:H buffer layer at the p/i interface and band gap profiling of the absorption layer on enhancing cell parameters in hydrogenated amorphous silicon germanium solar cells



Duy Phong Pham^a, Sangho Kim^b, Jinjoo Park^a, Jaehyun Cho^b, HyunSung Kim^a, Anh Huy Tuan Le^a, Junsin Yi^{a,*}

^a College of Information and Communication Engineering, Sungkyunkwan University, Suwon 440-746, Republic of Korea

^b Department of Energy Science, Sungkyunkwan University, Suwon 440-746, Republic of Korea

ARTICLE INFO

Article history:

Received 2 December 2016

Accepted 21 February 2017

Keywords:

Thin film solar cells

Buffer layer

Band gap profiling

ABSTRACT

Separate influences of a hydrogenated amorphous silicon (a-Si:H) buffer layer at the p/i interface and staircase band gap profiling of entire absorption layer on cell parameters, such as open-circuit voltage (V_{oc}), short-circuit current density (J_{sc}) and fill factor (FF), of hydrogenated amorphous silicon germanium (a-SiGe:H) thin film solar cells are discussed. An added thin a-Si:H buffer layer at the p/i interface can mainly improve V_{oc} and J_{sc} while the staircase band gap profiling can enhance FF. Consequently, a combination of the buffer layer and band gap profiling can lead to significantly enhance V_{oc} , J_{sc} and especially FF. A significant performance-improvement of the a-SiGe:H solar cell from 8.3% up to 9.8% was recorded by this combination. Role of the buffer layer and band gap profiling process was examined by empirical results and simulations.

© 2017 Elsevier GmbH. All rights reserved.

1. Introduction

The most essentially persistent pursuit in thin film silicon solar cells for competitive photovoltaic applications have focused on further enhancing the performance and stability [1]. All efforts have tended to multi-junction designs, in which the highest performance has been obtained for triple-junction designs [2,3]. In these structures, hydrogenated amorphous silicon germanium (a-SiGe:H) thin film solar cells mainly play a role as middle sub-cells, along with hydrogenated amorphous silicon (a-Si:H) top cells and microcrystalline silicon (μ c-Si:H) bottom cells. Further efficiency enhancement of these structures is supposed to further improving the quality of individual single junction thin film solar cells. In a-SiGe:H thin film solar cells, it has been well-known that an efficiency improvement can be caused by using different buffer layers (BLs) at the p/i or i/n interface and appropriate band gap profiling (BGP), the so-called band gap grading [4–7]. However, there have been different observations about effect of BLs and BGP on cell performance. D. Luntszien et al. showed that the complex band-gap grading technique can be replaced simply by using appropriately thin a-Si:H buffer layers at both interfaces [8,9]. In other aspects, B. Samanta et al. indicated that the light-induced degradation was faster in cells with buffer layers at the p/i interface; and they also proposed that for the absolutely highest stabilized efficiency of the double-junction cell, the buffer layer at the interface should be set at the top cell only [10]. Moreover, S. Guha et al. [11] and V. Dalal et al. [12] showed opposite observations

* Corresponding author.

E-mail addresses: pdphong@skku.edu (D.P. Pham), junsin@skku.edu (J. Yi).

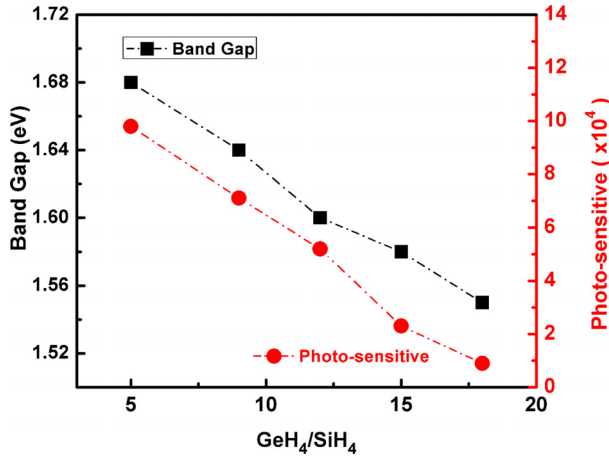


Fig. 1. Opto-electrical properties of single a-SiGe:H layers with various GeH₄/SiH₄ gas ratios.

about effect of the reverse profiling on fill factor parameter. As a result, effect of BLs and BGP on cell parameters of a-SiGe:H solar cells is still debates.

In this work, we experimented separately an a-Si:H buffer at the i/n interface and BGP of narrow-gap a-SiGe:H solar cells, and showed separate roles of the buffer and BGP on the a-SiGe:H cell parameters. In addition, a combination of both BL and BGP in a-SiGe:H cell structure is proposed as a favorable design for further cell efficiency enhancement.

2. Experiment

Plasma enhanced chemical vapor deposition (PECVD) cluster system with multi-chamber at the 13.56 MHz RF power source was used for cell fabrication. The single junction a-SiGe:H thin film solar cells in the p-i-n superstrate configuration were fabricated on the commercial FTO coated glass. An aluminum-doped zinc oxide (AZO) thin layer of 30 nm was coated on the FTO surface by sputtering system to protect the FTO electrode layer under bombardment of hydrogen plasma during preparation. Double p-type layers were used including a hydrogenated microcrystalline silicon oxide (p-μc-SiO_x:H) and an amorphous silicon oxide (p-a-SiO_x:H), which directly contacts with the front FTO electrode and intrinsic layer, respectively. N-type layers were hydrogenated microcrystalline silicon (n-μc-Si:H) layers. Intrinsic a-SiGe:H layers (i-a-SiGe:H) were deposited by adding germane (GeH₄) gas, beside silane (SiH₄) and hydrogen (H₂) reactant gases. Band gap profiling of the i-a-SiGe:H layers was implemented by controlling the band gap of the intrinsic layers, i.e. controlling [GeH₄/SiH₄] gas ratios, as equal staircase profiles of five steps during deposition. The band gap of the graded i-a-SiGe:H layers was gradually increased from 1.55 eV at the p-side to 1.68 eV at the n-side. The total film thickness of the i-a-SiGe:H layers was 300 nm.

Optical properties of the i-a-SiGe:H layers with and without band gap grading were examined by Fourier transform infrared spectroscopic (FT-IR) and spectroscopic ellipsometry (VASE®, J. A. Woollam). Electrical properties such as dark- and photo-conductivity of the i-a-SiGe:H layers (300 nm) with various optical band gap, as shown in Fig. 1, were examined in an aluminum co-planar electrode configuration using a programmable Keithley 617 electrometer. The current density-voltage (J-V) curve characteristics of the cells were tested in both standard dark and illumination conditions using AM 1.5 illumination. The band diagrams were simulated from the amorphous semiconductor analysis (ASA) simulation program.

3. Results and discussion

Apart from the optimization of the p- and n-type doped layers, which were published elsewhere by our group [13,14], quality of absorption a-SiGe:H layer is one of the important factors, which can affect strongly cell performance. Fig. 1 shows optoelectronic properties of the single a-SiGe:H layers with various optical band gaps, i. e. different Ge contents. It shows that the photosensitive, ratio of photo-conductivity to dark-conductivity, of these layers is in orders of 10⁴. Such ranges of the photosensitive are already in the acceptable values, characterizing the appropriate quality of the photon-absorption layers in thin film cell structures [15,16]. The structural schemata of the p-i-n a-SiGe:H solar cells with varying a-Si:H BLs at the p/i interface and BGP process of entire absorption layer are shown in Fig. 2. In these diagrams, cell A has a constant band gap absorption layer of 1.55 eV without any buffers at the p/i interface while cell B has an a-Si:H buffer of 15 nm at the p/i interface. Cell C has the staircase BGP while at cell D, an a-Si:H buffer layer at the p/i interface is combined to the staircase BGP. The J-V curves under 1 sun illumination of the cells are shown in Fig. 3. Cell parameters including open circuit voltage (V_{oc}), short circuit current (J_{sc}), fill factor (FF) and efficiency (E_{ff}), extracted from the J-V curve data, are presented in Table 1. The results show that the V_{oc} and J_{sc} of cell B and D, compared with that of cell A and C respectively, can be significantly increased by adding the a-Si:H BL at the p/i interface. In comparison between cells with and without band gap profiling, it can be seen that cells with band gap profiling, such as cell C and D, show higher FF than ones without profiling, cell A and B. In

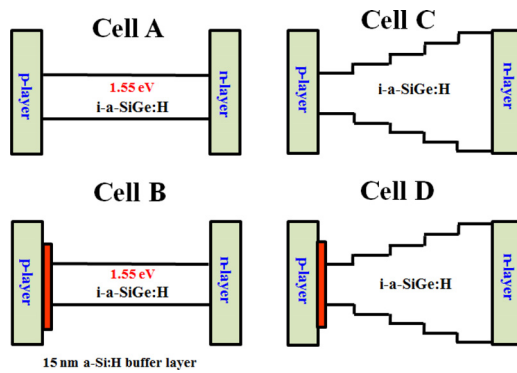


Fig. 2. Schematic diagram of cell structures with a-Si:H buffers at the p/i interface and band gap profiling.

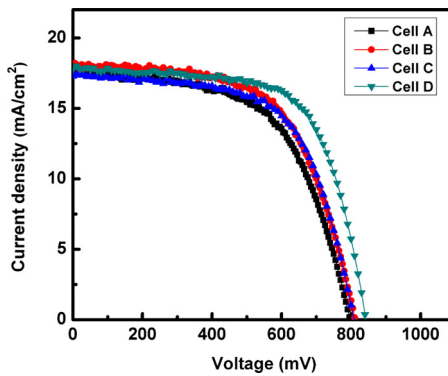


Fig. 3. J-V curve characteristics under standard illumination of a-SiGe:H solar cells.

Table 1

Cell parameters including V_{oc} , J_{sc} , FF and E_{ff} under light condition of a-SiGe:H solar cells.

Cell	Characteristic	V_{oc} (V)	J_{sc} (mA/cm ²)	FF (%)	Eff (%)
A	Constant Band Gap	0.79	17.5	60	8.3
B	Constant Band Gap + Buffer	0.81	18.2	61	9.0
C	Band Gap Profiling	0.8	17.3	63	8.7
D	Band Gap Profiling + Buffer	0.84	17.8	66	9.8

particular, it should be noticed that cell D with the combination of the a-Si:H BL and the staircase BGP shows a considerable enhancement in both the V_{oc} and FF, which lead to improve the cell performance up to 9.8%, as shown in Table 1.

It has been proposed that the recombination losses in bulk of the intrinsic layer as well as at both interfaces is directly responsible for the V_{oc} and FF parameters [17]. In order words, the defect state density in the absorption layer and at both interfaces strongly influences on the V_{oc} and FF. To individually examine influences of the BGP on the defect state density, two single absorption a-SiGe:H layers of 300 nm thickness with and without BGP were examined by FTIR spectra measurement and spectroscopic ellipsometry. Fig. 4a shows the imaginary-part characteristic of the dielectric constant $\langle \varepsilon_2 \rangle$ with photon energy of two films. It can be seen that the $\langle \varepsilon_2 \rangle$ spectra of the films indicate a broad single peak which represents the amorphous phase [18]. In addition, it should be noticed that the $\langle \varepsilon_2 \rangle$ spectrum peak of the sample with BGP process, as in cell C, shifts to higher photon energy range. This shift is attributed to the increase in the band gap of the intrinsic layer [18,19]. The low band gap of 1.55 eV of absorption layer as cell A is due to the high Ge content incorporation throughout entire absorption layer. While, the gradually reduced distribution of Ge content from p-side to n-side in graded film as cell C can cause the increase of the band gap. The Fourier Transform Infrared Spectroscopy (FTIR) has been well-known as the simple tool to evaluate the density of micro-voids through detecting vibrational modes of (polar) bonds [20]. In this study, the proofs from FTIR spectra, as shown in Fig. 4b, in comparison between single layers with and without BGP, show that there is a considerable decrease in the intensity of the absorption peak centered around 883 cm⁻¹, which attributed to the bending modes of dihydride bondings (Si-H₂) or polysilane (Si-H₂)_n [21]. In FTIR spectra of a-Si:H thin film, it has been well-known that two broad prominent peaks, centered at 640 and 2000 cm⁻¹, are attributed to the wagging and stretching mode, respectively, of the Si-H bonding. The others centered around 884 and 2100 cm⁻¹ characterize the bending and stretching mode of the Si-H₂ bonding [21,22]. It has been widely proposed that the high density of the Si-H₂ or (Si-H₂)_n bonding, which ascribed to micro-voids; i.e. porosity, defects in film structure, is assigned to poor quality of the amorphous silicon thin film

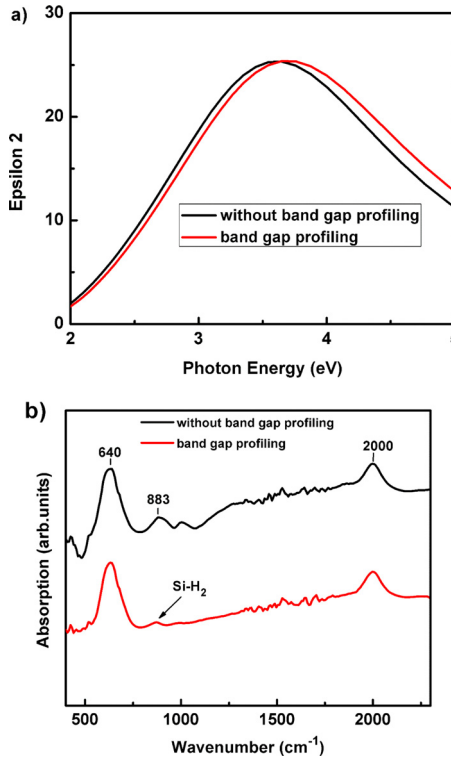


Fig. 4. a) Variation of epsilon 2 spectra with photon energy and b) FTIR absorption spectra of single a-SiGe layers with and without band gap profiling.

[21–23]. Thus, the significant decrease in the intensity of the Si-H₂ bending modes around 884 cm^{-1} , as shown in Fig. 4b, is associated to better improved quality of the a-SiGe:H single layer with profiling process. In summary, the profiling process by combining the optimized different band-gap layers, as shown in Fig. 1, results in the reduction in the defect status density of absorption layer.

Smoothing a band gap discontinuity at both interfaces, the p/i and i/n interfaces, has been proposed as a favorable factor for improving cell performance. D. Lundszien et al. [8,9] experimentally showed that the thin a-Si:H buffer layer at the p/i interface can increase V_{oc} while detrimental FF. In addition, B. Samanta et al. [10] proposed that the a-SiC:H constant band gap buffer layer at the p/i interface of the a-Si:H solar cells can reduce interface defects and thus improved the V_{oc} and J_{sc} . Moreover, F. Smole et al. [24] suggested that the band gap grading at the p/i interface can reduce interface states as well as carrier losses and thus enhance the V_{oc} . Furthermore, the influence on either the V_{oc} or J_{sc} caused by varying the grading width at the p/i interface in the a-SiGe:H cells were also recorded by R. A. C. M. M Van Swaaij et al. [25] throughout both simulation and experiment. It showed that the lowered optical band gap, i. e. high Ge content incorporation in active a-SiGe:H layer, can cause the band gap discontinuity and high defect density at the p/in interface [26]. These can adversely affect the carrier extraction, especially the hole extraction, and the internal electric field [8,9]. To illustrate separate role of the a-Si:H BL at the p/i interface, we used the ASA simulation program to simulate the cell operations. This program is a one-dimensional device simulator tool. It was designed for the simulation of the amorphous silicon solar cell operation [27]. Band diagrams of cell A, B, C and D, extracted from this program, are illustrated in Fig. 5. A high potential barrier, which can considerably hinder the hole collection, is formed at the p/i interface of cell A and C, without BL. This high barrier can be formed due to significant difference of the optical band gap between the p-type layers (over 1.9 eV) and the intrinsic a-SiGe:H layer (1.55 eV) [9,28]. The added a-Si:H BL, with the intermediate optical band gap of around 1.75 eV, as in cell B, can lower this barrier, and thus result in better hole collection. In particular, it should be noticed that this barrier is significantly lowered by combining the BGP and the BL as in cell D. This can lead to more efficient hole extraction. Consequently, it can be concluded that the a-Si:H BL at the p/i interface plays an important role in reducing the band discontinuity, so called the band-offset, between the high band gap p-type doped layers and the low band gap a-SiGe:H absorption layer. This smoothing can help for better hole extraction and thus enhance the V_{oc} and FF. To demonstrate distinctly these points, the dark I-V curve characteristics of the cells were examined in the standard dark condition. Cell parameters including ideal diode factor (n), R_s and J_o , extracted from this dark data [29], are expressed in Fig. 6. The detail values of these parameters are shown in Table 2. It shows clearly in Table 2 that the J_o and R_s of cell B and D, with BL, are apparent lower than that of cell A and C, respectively. It is possible that the high potential barrier at the p/i interface can cause the accumulation or recombination of the photo-generated carriers, especially hole collection, and thus result in the high R_s value as well as the J_o . Consequently,

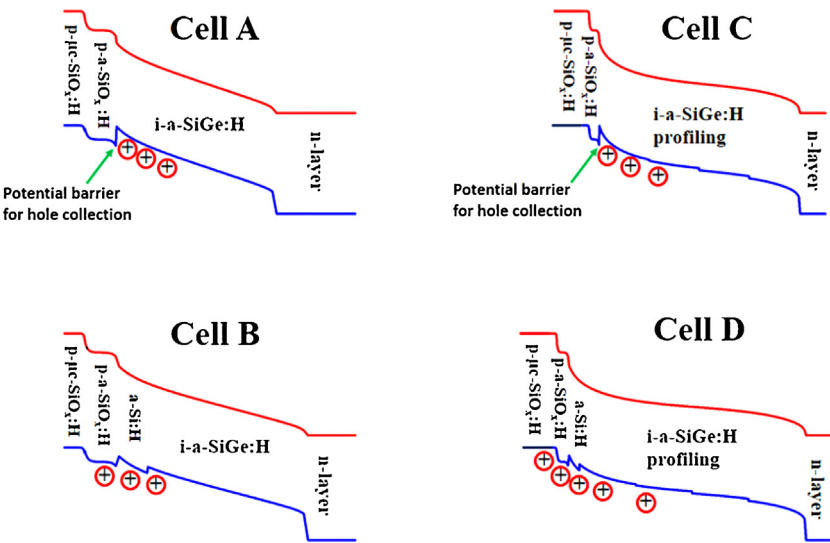


Fig. 5. Band diagrams extracted from ASA simulation of a-SiGe:H solar cells.

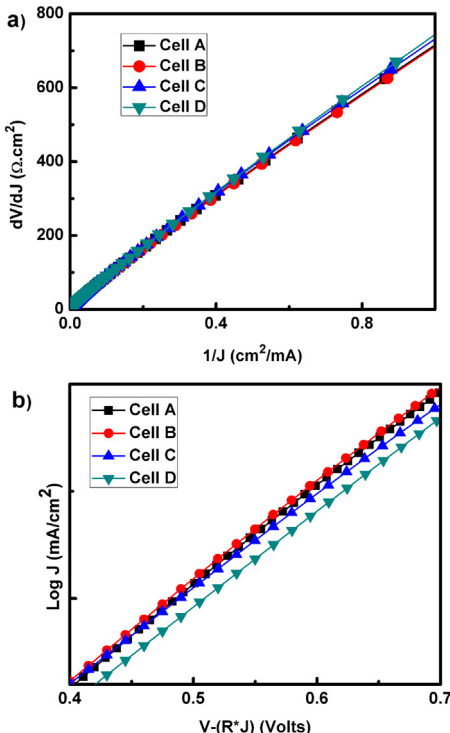


Fig. 6. Characteristics from dark $J(V)$ measurement including a) dV/dJ versus $1/J$ of cells (intercept is R_s); and b) $\log J$ as a function of $V - (R^*J)$, (intercept is J_0).

the a-Si:H BL, as in cell B and D, is possible to a favorable choice for reducing the band-offset, and extracting better the carriers.

The band gap profiling of a-SiGe:H thin film solar cells was early suggested by S. Guha's group [11]. They indicated that the "normal" profiling of a-SiGe:H solar cells improved the V_{oc} and FF while the "reverse profiling" further enhanced V_{oc} and J_{sc} . Consequently, a combination of the "reverse" profiling at the p/i interface and the "normal" grading of absorption layer revealed a significant cell performance [11]. Regarding other aspects, several groups have been focused on smoothing the p/i and i/n interfaces. Typically, D. Lundszen et al. [8,9] concluded that the band gap profiling at both interfaces of the narrow-gap a-SiGe:H solar cells can be simply replaced by an a-Si:H buffer layer. In comparison, we find that the a-Si:H BL at the p/i interface can improve the V_{oc} and J_{sc} while the BGP can enhance the FF. Consequently, the combination of the

Table 2

Diode parameters including the ideal diode factor (n), inverse saturation current density (J_o) and series resistance (R_s) extracted from dark I-V curve characteristics.

Cell	Characteristic	n	J_o (mA/cm ²)	R_s (Ω cm ²)
#1	Constant Band Gap	1.6	1.5×10^{-7}	9
#2	Constant Band Gap + Buffer	1.6	1.1×10^{-7}	8.4
#3	Band Gap Profiling	1.7	1.2×10^{-7}	8.5
#4	Band Gap Profiling + Buffer	1.7	7.9×10^{-8}	7.5

buffer and the BGP is chosen, in this study, for further cell efficiency improvement. It is apparent that the cell performance is considerably enhanced from 8.3% to 9.8% by this design, as shown in Table 1. As a results, this design is expected as the motivation, which is comparable to the other advantaged designs as U-, V- and E-shapes [9,30,31].

4. Conclusion

We examined, in comparison, the influences of an a-Si:H buffer layer at the p/i interface and staircase band gap profiling of entire a-SiGe:H absorption layer on cell parameters of the narrow-gap a-SiGe:H thin film solar cells. The staircase band gap profiling of entire a-SiGe:H absorption layer can reduce the defect status density in bulk, limit the carrier recombination loss and thus result in elevating FF. The a-Si:H buffer layer with the intermediate band gap at the p/i interface can play essential roles in smoothing the band discontinuity, band-offset, between the p-layers and the low-gap intrinsic a-SiGe:H layers, promote hole extraction, and thus lead to elevating V_{oc} and J_{sc} . In particular, the cell with the combination of both the buffer and band gap profiling shows significant enhancement in V_{oc} , FF and J_{sc} , which results in the significant cell efficiency improvement from 8.3% to 9.8%. Consequently, a combination of buffer layer and BGP is proposed as a favorable design for further cell efficiency enhancement.

Acknowledgments

This research was supported by the New & Renewable Energy Core Technology Program of the Korea Institute of Energy Technology Evaluation and Planning (KETEP), granted financial resource from the Ministry of Trade, Industry & Energy, Republic of Korea (No. 20163010012230).

References

- [1] T. Matsui, M. Kondo, Sol. Energy Mater. Sol. Cells 119 (2013) 156–162.
- [2] S. Kim, J.W. Chung, H. Lee, J. Park, Y. Heo, H.M. Lee, Sol. Energy Mater. Sol. Cells 119 (2013) 26–35.
- [3] B. Yan, G. Yue, L. Sivec, J. Yang, S. Guha, C.S. Jiang, Appl. Phys. Lett. 99 (2011) 113512.
- [4] J. Zimmer, H. Stiebig, H. Wagner, J. Appl. Phys. 84 (1998) 611.
- [5] R.J. Zambrano, F.A. Rubinelli, W.M. Arnoldbik, J.K. Rath, R.E.I. Schropp, Sol. Energy Mater. Sol. Cells 81 (2004) 73–86.
- [6] B. Liu, L. Bai, J. Ni, H. Zhao, C. Wei, J. Sun, Y. Zhao, X. Zhang, Adv. Optoelectron. Energy Environ. (2013), ASu 3A.7.
- [7] F.A. Rubinelli, R. Jimenez, J.K. Rath, R.E.I. Schropp, J. Appl. Phys. 91 (2002) 2409.
- [8] D. Lundszien, F. Finger, H. Wagner, Sol. Energy Mater. Sol. Cells 74 (2002) 365–372.
- [9] D. Lundszien, F. Finger, H. Wagner, Appl. Phys. Lett. 80 (2002) 1655.
- [10] B. Samanta, D. Das, A.K. Barua, Sol. Energy Mater. Sol. Cells 46 (1997) 233–237.
- [11] S. Guha, J. Yang, A. Pawlikiewicz, T. Glatfelter, R. Ross, S.R. Ovshinsky, Appl. Phys. Lett. 54 (1989) 2330.
- [12] V. Dalal, SERI Semiannual Subcont Report, 198717–23.
- [13] C. Shin, S.M. Iftiqar, J. Park, S. Ahn, S. Kim, J. Jung, S. Bong, J. Yi, Mater. Chem. Phys. 159 (2015) 64–70.
- [14] J. Park, C. Shin, S. Lee, S. Kim, J. Jung, N. Balaji, V.A. Dao, Y.J. Lee, J. Yi, Thin Solid Films 587 (2015) 132–136.
- [15] B. Yan, L. Zhao, B. Zhao, J. Chen, G. Wang, H. Diao, Y. Mao, W. Wang, Vacuum 89 (2013) 43–46.
- [16] J. Xu, S. Miyazaki, M. Hirose, J. Non-Cryst. Solids 208 (1996) 277–281.
- [17] R.J. Zambrano, F.A. Rubinelli, W.M. Arnoldbik, J.K. Rath, R.E.I. Schropp, Sol. Energy Mater. Sol. Cells 81 (2004) 73–86.
- [18] Z. Tang, W. Wang, D. Wang, D. Liu, Q. Liu, M. Yin, D. He, Appl. Surf. Sci. 256 (2010) 7032–7036.
- [19] M.K. Khan, L.K. Malhotra, S.C. Kashyap, J. Appl. Phys. 66 (1989) 2528.
- [20] M. Zeman, I. Ferreira, M.J. Geerts, J.W. Metselaar, Sol. Energy Mater. 21 (1991) 255–265.
- [21] G.H. Wang, C.Y. Shi, L. Zhao, R.D. Hu, L.L. Li, G. Wang, J.W. Chen, H.W. Diao, W.J. Wang, Thin Solid Films 552 (2014) 180–183.
- [22] D.Y. Kim, I.A. Yunaz, S. Kasashima, S. Miyajima, M. Konagai, Sol. Energy Mater. Sol. Cells 95 (2011) 829–837.
- [23] B. Drevillon, F. Vaillant, Thin Solid Films 124 (1985) 217–222.
- [24] F. Smole, J. Furlan, S. Amon, 5th Int Photovoltaic Sci. Eng. Conf. (1990) 335.
- [25] R.A.C.M. van Swaaij, M. Zeman, S. Arnoult, J.W. Metselaar, Proc. 28th IEEE PV Specialist Conf. (2000) 869–872.
- [26] H.J. Hsu, C.H. Hsu, C.C. Tsai, J. Non-Cryst. Solids 358 (2012) 2277–2280.
- [27] K.R. Kumar, M. Zeman, Bull. Mater. Sci. 31 (2008) 737–739.
- [28] J. Fang, Z. Chen, N. Wang, L. Bai, G. Hou, X. Chen, C. Wei, G. Wang, J. Sun, Y. Zhao, X. Zhang, Sol. Energy Mater. Sol. Cells 128 (2014) 394–398.
- [29] S.S. Hegedus, Prog. Photovolt. Res. Appl. 5 (1997) 151–168.
- [30] R.J. Zambrano, F.A. Rubinelli, J.K. Rath, R.E.I. Schropp, J. Non-Cryst. Solids 299–302 (2002) 1131–1135.
- [31] J.W. Chung, J.W. Park, Y.J. Lee, S.W. Ahn, H.M. Lee, O.O. Park, Jpn. J. Appl. Phys. 51 (2012) 10nb16.